Electrochemical Assessment Accounting for the Interaction of Chalcopyrite/Xanthate System

E.D. Moreno-Medrano[1,], N. Casillas[2], E.R. Larios-Durán[2], R. Cruz[3], R. H. Lara[4],*
A. Carreon-Alvarez[5], A. Gutierrez-Becerra[6], M. Bárcena-Soto[2], M.A. Pedroza-Toscano[1]

[1]University Center UTEG, Gdl. 44430, Mex.
[2]Department of Chemistry, UdeG, Gdl. 44430, Mex.
[3]Institute of Metallurgy, UASLP, SLP.78210, Mex.
[4]Department of Material Science, FCQ, UJED, Dgo. 34120, Mex.
[5]University Center of Valles, UdeG, Gdl. 46600, Mex.
[6]University Center of Tonala, UdeG, Gdl. 48525, Mex.
[*]E-mail: david.moreno@uteg.edu.mx

In the current work cyclic voltammetry, capacitance associated to double-layer and Electrochemical Impedance studies on chalcopyrite surfaces in absence and occurrence of Na-isopropyl xanthate at highly concentrated medium in an extensive range of polarization potentials are examined. The voltammetric response of the chalcopyrite surface displays a passivating effect with the addition of xanthate due to its adsorption, which also impedes the transport of oxidized species Fe^{2+} and Cu^{2+} outwards the mineral matrix. A large surface amendment of the chalcopyrite interface at highly thiocollector concentration solutions also becomes evident by analyzing the capacitance-potential curves for different xanthate concentration. Potential Zero Charge (PZC) measurement of the system is equal to 0.2 V vs. SCE and it matches with the adsorption and oxidation potential of xanthate (X^-) on the chalcopyrite sample. In addition, impedance spectra being acquired at the passivating region, denotes a pseudocapacitive effect of the system, consistent with the xanthate adsorption and blocking species at the interface. Finally, impedance spectra present three time constants attributed to the oxidative process of chalcopyrite and X^- and the formation of covellite and cuprous xanthate on the surface of the mineral, which are in agreement with the voltammetric response obtained for the system.
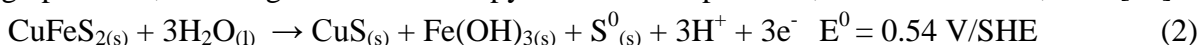
1. INTRODUCTION

Historically copper production has relied heavily on exploitation of secondary sulfides, such as: chalcocite (Cu_2S), bornite (Cu_5FeS_4) and covellite (CuS). However, a worldwide overexploitation of sulfides has substantially contributed to its depletion; thus mining companies have started looking at

other viable alternatives for exploitation, such as polymetallic deposits rich in chalcopyrite ($CuFeS_2$). On this circumstances chalcopyrite is becoming one of the most commonly mined ores for copper extraction in numerous countries. In the case of Mexico, the chalcopyrite appears predominantly as porphyry copper deposits distributed in different mines across the country; one of them is Cananea (recognized worldwide) and La Caridad; and, in fields where mineralization occurs even more disseminated, as occurs in Charcas, San Luis Potosi and Santa Barbara, Chihuahua. On the other hand, to make the smelting operations process more efficient, it is normally required that low concentration $CuFeS_2$ undergo a pre-concentration processes by flotation with the uses of depressants and collectors.

Since flotation is one of the most preferred enrichment techniques for ores with different compositions, e.g., Pb-Zn-Cu, Cu-Pb, it has been subjected to a large number of studies [1-10]. Although flotation involves several chemical interactions between the minerals and surface agents most of the reactions are electrochemical in nature. For instance, there is an electrochemical interaction between chalcopyrite-xanthate, which takes place via a complex mechanism where the anodic reactions involve the oxidation of the mineral and collector. Along with these reactions other natural occurring process takes place, such as oxygen reduction reaction. In the sake of a brief remainder of the processes, we can mention that Allison et al. [11] reported that one of the products of these interactions is the formation of dixanthogen. Further studies by Richardson et al., [12] and Roos et al., [13-14] have demonstrated that there is reasonable flotation process of the $CuFeS_2$, below the revocable potential for formation of dixanthogen compounds. According to these findings, it was associated with the formation of surface compound, namely cuprous xanthate:

$$CuFeS_{2(s)} + X^-_{(l)} \rightarrow CuX_{(s)} + FeS_{2(s)} + e^- \qquad\qquad E^0 = -0.096 \text{ V/SHE} \qquad (1)$$
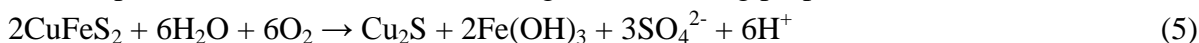
By following Leppinen et al., [15] work, he demonstrated by FTIR studies that cuprous xanthate is produced near to the dixanthogen forming potential. The formation of CuX takes place at very high potential, evolving from the chalcopyrite oxidation products, such as covellite, CuS [15]:

$$CuFeS_{2(s)} + 3H_2O_{(l)} \rightarrow CuS_{(s)} + Fe(OH)_{3(s)} + S^0_{(s)} + 3H^+ + 3e^- \quad E^0 = 0.54 \text{ V/SHE} \qquad (2)$$

$$CuS_{(s)} + X^-_{(l)} \rightarrow CuX_{(s)} + S^0_{(s)} + e^- \qquad\qquad E^0 = -0.11 \text{ V/SHE} \qquad (3)$$

The oxidation of xanthate and subsequent formation of dixanthogen is described by the following reaction [3, 16-17]:

$$2X^-_{(l)} \rightarrow X_{2(l)} + 2e^- \qquad\qquad E = -0.06 - 0.059 \log [X^-] \qquad (4)$$

In a more recent work by Mustafa et al., [18], they proposed that chalcopyrite-xanthate interactions for pH between 8 and 10 occur through the following proposed reactions:

$$2CuFeS_2 + 6H_2O + 6O_2 \rightarrow Cu_2S + 2Fe(OH)_3 + 3SO_4^{2-} + 6H^+ \qquad (5)$$

$$Cu_2S + 2X^- + 2O_2 \rightarrow 2CuX + SO_4^{2-} \qquad (6)$$

This contribution addresses the interfacial reactions at the chalcopyrite surface produced by scanning the potential in absence or presence of xanthate. Some of the oxidation-reduction and adsorption-desorption reactions above mentioned are supported with double layer differential capacitance and EIS measurements. Both experimental results and their interpretation are in agreement with published data and new insights into a better understanding of the chalcopyrite-xanthate interface, critical for the flotation processes, are provided.

2. EXPERIMENTAL

Electrochemical experimentations were performed using a typical three-electrode cell. Native chalcopyrite crystals were obtained from Charcas, San Luis Potosí (México). These samples were handly selected to transform into mineral coupons for massive chalcopyrite electrodes (MCE) construction, involving exposed electrode area of *c.a.* 1.4 cm^2. Crystal samples were mineralogically characterized with atomic absorption spectroscopy (AAS), scanning electron microscopy with chemical analysis (SEM-EDS) and X-ray diffraction patterns (XRD). A typical purity essay of the working electrode was of 98.5% with 1.44% pyrite, 0.039% sphalerite and Ag and Sb traces. It was used a graphite rod (0.65 cm diameter) as counter electrode and a Saturated Calomel Electrode (SCE, 0.24 V vs. SHE) as reference electrode. For each experiment, the MCE surface was renewed by polishing until reach a mirror-like condition using alumina suspension (5 μm). None initiation surficial process was applied to the MCE. The characterization medium comprised an aqueous xanthate solution at diverse concentrations (i.e., 0, 1, 10 and 100 mM) added as Na isopropyl xanthate (Alkemin) with 0.01M KCl at pH 8 (Fermont) included as supporting electrolyte. High-quality deionized water (18 MΩ Barnstead D4641) was used for preparation of all solutions during experiments and the chemical reagents were used as received without additional purification. An inert atmosphere (N$_2$) was kept during course of electrochemical experiments, and the temperature was maintained at 25 °C.

Cyclic voltammetry measurements were conducted using a Solartron SI 1287 potentiostat/galvanostat and data were acquired by software Coreware$^®$. Potential range of -1.2 to 1.2 V was selected during voltammetric experiments at 10 mV·s^{-1}. Before each experiment, open circuit potential (OCP, where current is zero) was monitored until minimal changes were observed. Voltammetric scans were initiated into positive-going direction and direction changed from positive to negative-going scans for all cases. Electrochemical impedance spectroscopy (EIS) and capacitance analyses were performed using a Solartron 1260 FRA module coupled to a Solartron SI 1287 potentiostat and/or an A/D data gaining card model NI PCI-6251, home-based software and a Pine Instruments AFCBP1 potentiostat/galvanostat.
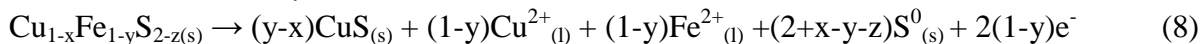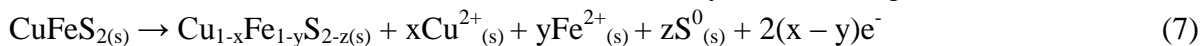
Double-layer capacitance experiments were obtained by EIS using a constant frequency (1 kHz), different polarization range (from -1.2 V to 1.2 V vs. SCE) and 10 mV·s^{-1}. Additionally, EIS experiments were carried out using a wave signal of ± 10 mV, 20 kHz to 2 mHz as frequency range and seven points per decade. EIS experimental data (Nyquist diagrams) were analyzed using equivalent circuits procedure by software Zplot$^®$. All EIS experiments were performed after reached stable OCP conditions (± 20 mV), thus avoiding current variations and assuring a steady state for EIS acquisition data. It is worth noting that in all cases, the real impedance was normalized by subtracting the solution resistance of the total impedance.

3. RESULTS AND DISCUSSION

3.1 Cyclic Voltammetry

Typical cyclic voltammograms for chalcopyrite system at different switching potentials, E$_{\lambda+}$ of 1200 mV, 1000 mV, 800 mV and 600 mV are shown in Fig. 1a. The voltammograms are

characterized by an oxidation reaction (peak O1) appearing as a current wall that relies on the massive mineral oxidation, a process only controlled by charge transfer. According to Yin et al, [19] the peak O1 includes both the oxidation of chalcopyrite that leaves a copper, iron and sulfur deficient surface and the formation of covellite, CuS, that can be summarized by the following reactions:

$$CuFeS_{2(s)} \rightarrow Cu_{1-x}Fe_{1-y}S_{2-z(s)} + xCu^{2+}{}_{(s)} + yFe^{2+}{}_{(s)} + zS^0{}_{(s)} + 2(x-y)e^- \tag{7}$$

$$Cu_{1-x}Fe_{1-y}S_{2-z(s)} \rightarrow (y-x)CuS_{(s)} + (1-y)Cu^{2+}{}_{(l)} + (1-y)Fe^{2+}{}_{(l)} + (2+x-y-z)S^0{}_{(s)} + 2(1-y)e^- \tag{8}$$

The cathodic current peaks R1 and R2 diminish while decreasing, E_λ, suggesting that reduced species come from the oxidized products previously generated in O1. To further investigate the nature of this species, we proceed to stir the media (Figure 1b), the reduction peak R1 decreases in size and the oxidation peak O2 completely disappears. Hence, all products generated in the oxidation peak O1 are soluble species that can be simply sweep away by stirring and cannot be detected for the reverse potential scan. In addition, the oxidized species in O2 correspond to reduced species in R1. Finally, since the reduction peak R2 virtually does not change, it is attributed to the reduction of chalcopyrite.
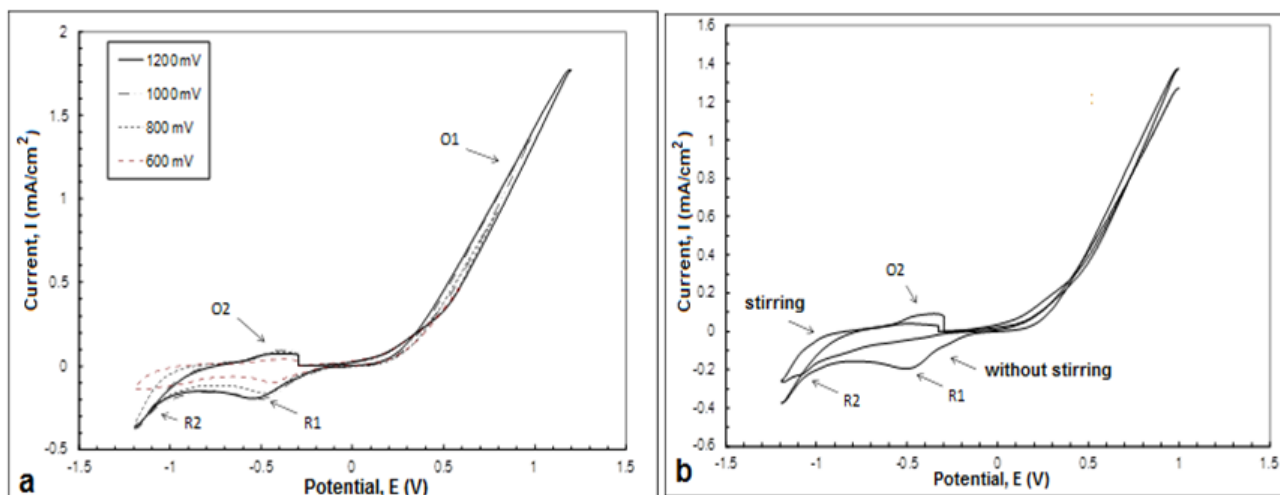
Figure 1. Cyclic voltammograms for chalcopyrite immersed in KCl 0.01 M solution. (a) Effects of variation of switching potential, E_λ. (b) Stirring effects. Scan rate= 20 mV s^{-1}.

By adding xanthate into the system the voltammetric response changes rather substantially. Figure 2a shows cyclic voltammograms of chalcopyrite for several xanthate concentrations. For sweeping potentials at low xanthate concentration, oxidation products at the surface rapidly evolve into other species through processes controlled solely by potential; this is evidenced by a current wall observed in the voltammograms for xanthate concentrations lower than 0.01 M. When the xanthate concentration increases, its effects become more evident; emerging several oxidation peaks. Now xanthate is adsorbed on the surface, limiting the transport of species from the mineral matrix to its surface and they are reactions controlled by both charge transfer and mass transport. On this basis, the oxidation peaks O1 and O2 are explained in terms of the reactions (7) and (8). The species generated in these reactions react with the adsorbed xanthate on the electrode surface producing cuprous xanthate and iron hydroxides, according to the following reaction [19-20]:

$$Cu_{1-x}Fe_{1-y}S_{2-z} + CuS + X^- \rightarrow CuX + Fe(OH)_3 + S° + 2e^- \qquad (9)$$
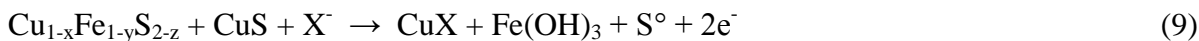
It has been fully established in the literature that xanthate absorption takes place via a charge transfer process, which involves its oxidation, adsorption and subsequent formation of dixanthogen species, described by reaction (4). These processes can be observed as an overlapping on peak O1 (Fig 2a). All proposed reactions depend on potential, according to the exchange of electrons. In addition, it takes place the oxidation of chalcopyrite according to reaction (7) at a potential of 0.27 V and both processes are involved in the oxidation peak O1. As previously mentioned, adsorption of X^- species on the chalcopyrite surface blocks the transport of species Fe^{2+} and Cu^{2+} from the mineral matrix to its surface, passivating it. Once the potential is moved toward more positive values the oxidation begins, forming covellite, CuS, reaction (8), oxidation peak O2. Finally, covellite reacts with the adsorbed X^- species on the mineral surface, promoting the formation of CuX and $Fe(OH)_3$, reaction (9), oxidation peak O3.

Research work regarding chalcopyrite oxidation under neutral-alkaline conditions indicates as initial step the conversion of chalcopyrite pristine surface to sulfur-rich metal deficient compounds comprising polysulfides (e.g., S_n^{2-} associated with $Cu_{1-x}Fe_{1-x}S_2$-like), covellite (CuS)-like, followed by soluble sulfur species generation (e.g. $S_2O_3^{2-}$, SO_4^{2-}), and Fe(III) precipitates such as K-jarosite ($Fe_3 \cdot (SO_4)_2(OH)_6$) [21-23]. The electrochemical formation of these secondary compounds could arise during the course of chalcopyrite oxidation in our system (Fig. 1a), whence EIS analysis aims to monitor adequate details during evolution of chalcopyrite-xanthate system.

3.2 Double-layer capacitance measurements

The mechanisms for X^- adsorption of and its relationship to the anodic oxidation of chalcopyrite were assessed by measuring the double-layer differential capacitance (DLDC). Double layer capacitance experiments as a function of the applied potential (polarization range from -1.2 to 1.2 V vs. SCE, in agreement with voltammetric analyses) for different X^- solutions are shown in Figure 2b. As it becomes evident, the values of the DLDC are lower in the absence of X^- than in its occurrence and methodically rise for larger collector concentrations. The variance between the profile and obtained values of the potential-capacitance results (DLDC curves) as a function of the X^- contains suggests a highlighted chemical amendment of the interface, being enabled by a high X^- concentration, as previously shown in voltammetric results (Fig. 1), for the potential interval registered. For a high X^- contains (i.e., 0.05 and 0.1 M), DLDC curves show a precise minimum at 0.2 V (Fig. 1b). According to the electrochemical double layer classical theory [24], the minimum at the V-shaped capacitance curves can be associated with the potential zero charge (PZC) for $CuFeS_2$-X^- system. In this respect, from the Potential Zero Charge (PZC) condition is feasible to envisage the potential interval where X^- adsorption is electrostatically more adequate in system. Since, X^- is anionic specie; its adsorptive process is more feasible on the mineral surface from 0.2 V and toward higher potentials. In addition, the V-shaped DLDC measurement can be explained in terms of the adsorption of organic species [25-26] and coincides with the potential (E, Volts vs SCE) where the adsorbed X^- is stable. Remarkably,

the PZC (0.2 V) coincides with the value of the starting potential for the oxidation peak O1 (Figure 2a).

At potentials above 0.4 V capacitance starts decreasing rapidly. By comparing the capacitance curves with the cyclic voltammograms (Fig. 2a), both coincide with an amendment of the chalcopyrite-X^- interface enabled by the electrochemical reaction (8). Thus, the surface passivation breaks down, at the end of peak O1, and oxidation starts over at the beginning of peak O2 (Fig. 2a). It should be emphasized that capacitance results are in agreement with the voltammetric analysis (Fig. 1a).
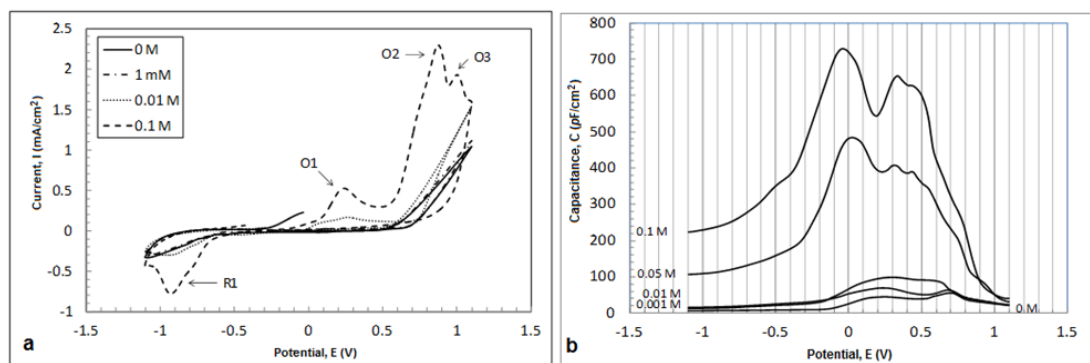

Figure 2. (a) Cyclic Voltammograms for chalcopyrite in presence of xanthate. (b) DLDC- potential response acquired at 1 kHz and 10 mV·s^{-1}.

3.3 Electrochemical Impedance Spectroscopy

The adsorption-desorption process of xanthate and its role in the electro-oxidation process of chalcopyrite was evaluated by EIS in absence and occurrence of X^- at concentrations of 0.1 M, to ensure that the adsorption of the X^- species are not insignificant. For this investigation the interval of the applied polarization potentials was around the Point of Zero Charge, PZC. Impedance spectra obtained for chalcopyrite in a 0.01 M KCl solution in the absence of xanthate are shown in Figure 3. From these results, we can detect that for all applied potentials (from -0.2 to 0.4 V vs. SCE), the shape of the spectra are quite similar. In general, we observe that for the entire frequency range investigated a purely capacitive behavior is observed due to the charging of the double-layer (DL). This EIS signal can be effectively symbolized by an equivalent electrical circuit which comprises a constant phase element (CPE1) attributed to a non-ideal capacitance of the DL in mineral/X^- system, occurring in parallel with a resistor (R2), associated to the charge transfer process in system. An additional resistance (R1) is included in series to represent the solution resistance. The equivalent circuit shown in Figure 4a was then fitted to the experimental Nyquist plot using the well-known Levenberg-Marquardt algorithm. Table I summarizes the obtained values of each parameter included in the fitted equivalent electrical circuits. The statistical error is suitable for all EIS fitted spectra with an x^2 in the order of 1x10^{-3}. Similar results are reported by Velásquez et al., [27].
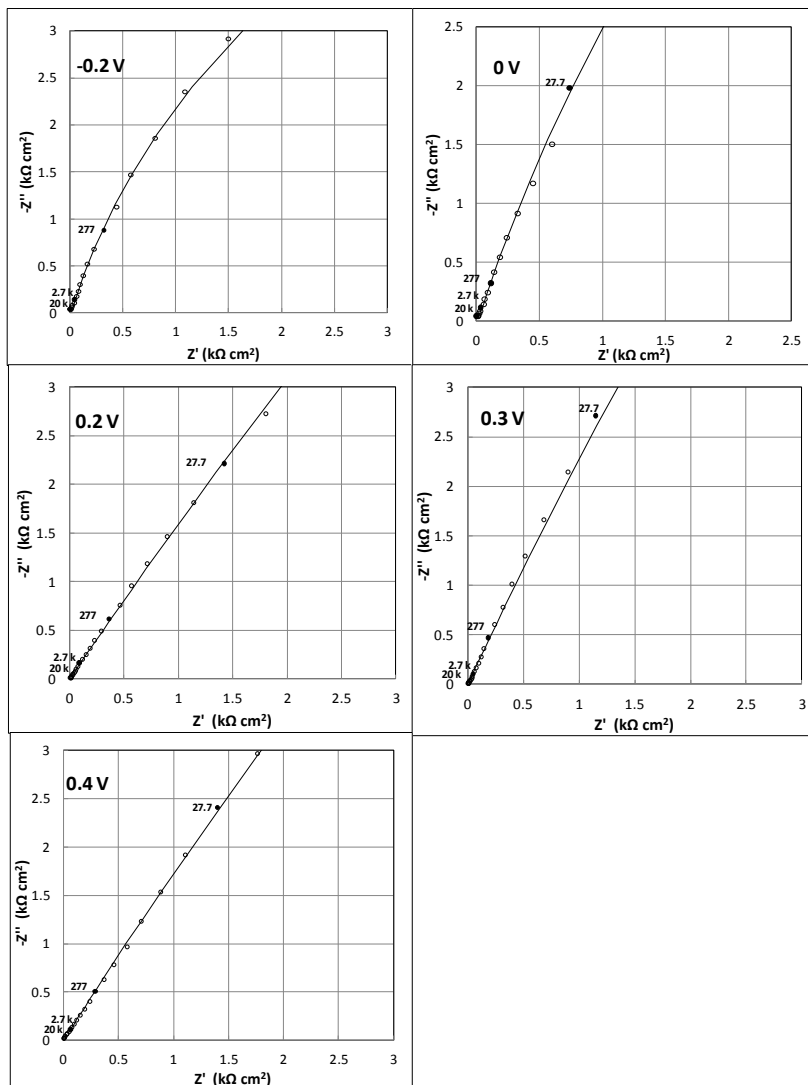
Figure 3. Complex EIS spectra (Nyquist plots) for chalcopyrite system (KCl 0.01 M solution at different polarization potentials). Experimental data is shown in open symbols (o). Fitted data is shown in continuous lines. Proposed equivalent circuits are shown in Figure 4a. Frequency in Hertz.
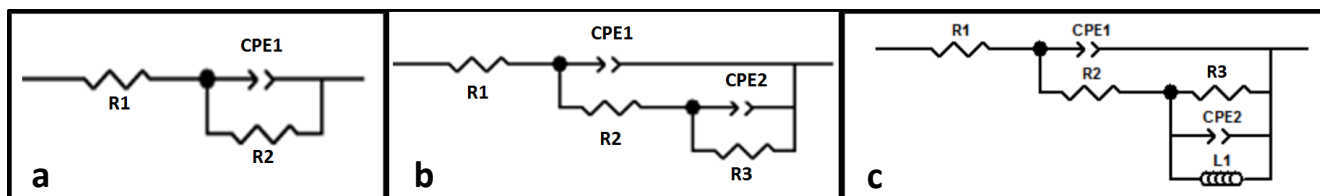
Figure 4. Proposed equivalent circuits arising from EIS spectra (Nyquist plots) data fitting for the chalcopyrite/electrolyte interface: (a) Equivalent circuit for chalcopyrite in 0.01 M KCl as reference. (b) Equivalent circuit for chalcopyrite/X⁻ system after MCE electrochemical oxidation at 0 V vs. SCE. (c) Equivalent circuit for chalcopyrite/X⁻ system after MCE electrochemical oxidation from 0.2 V to 0.4 V vs. SCE.

Table I. Parameters and values using in the equivalent circuit procedure associated to EIS data in Fig. 3a for chalcopyrite in absence of X^-.

E (V)	CPE ($\mu\Omega cm^{-2} s^n$)	n	$R_{CT1}(k\Omega)$
-0.2	3.6	0.829	14.52
0	3.2	0.815	31.2
0.2	39.2	0.622	110
0.3	24.5	0.746	108
0.4	26.4	0.674	95

On the other hand, to better understand the nature of the anodic chalcopyrite electro-oxidation in the occurrence of X^-, impedance spectra were obtained for the mineral-solution interface for potential polarization near the PZC. Figure 5 shows the impedance spectra obtained for chalcopyrite in the presence of xanthate at a concentration of 0.1 M. For the case of the spectrum obtained at a polarization potential of -0.2 V, it can be observed two time constants. The first one has been associated with the double layer charging and the second one to the incipient xanthate oxidation on the electrode surface. Both processes are represented by the equivalent circuit shown in Figure 4b. When the polarization potential is increased to 0 V, it appears an inductive loop explained in terms of the rearrangement of species due to the xanthate adsorption-desorption processes. Thus, the adsorbed xanthate behaves such as an intermediary adsorbed on the electrode surface. Moreover, the reduction of the charge transfer reaction (R_{CT1}) (observed in the low frequency range) indicates that oxidation and subsequent xanthate adsorption-desorption process is favored (Table II). These processes are taking into account in the equivalent circuit shown in Figure 4c. When the polarization potential is increased to 0.2 V the spectrum modifies significantly, in this particular case, it appears a well-defined loop at high frequencies correlated with the oxidation and adsorption of xanthate, reaction (4) and at low frequencies appears a typical Warburgh impedance element correlated with a diffusion controlled process. However, if we look at spectra obtained at higher potentials (0.3 and 0.4 V) the diffusional effect disappears, thus we ruled out a diffusion controlled process. To further support this, we can indicate that impedance measurements are carried out in highly concentrated xanthate solutions and it is a rather difficult to envision a diffusion controlled process. Instead, the time constant observed at the low frequency range (Fig. 5, 0.2 V) has been correlated with a pseudocapacitive effect on the system related to the passivation of the surface as was previously mentioned in the voltammograms (Figure 2a). We conclude that the spectrum has two time constants. One of them corresponds to the adsorption and oxidation of X^- species and the subsequent, at a very slow charge transfer process in the mineral-solution interface, correlated with the incipient oxidation of chalcopyrite, reaction (7). This behavior can be represented by the parallel coupling of a capacitor correlated with the double layer capacitance C_{dl} (CPE1) and a resistance associated with a charge transfer R_{CT1} (R2) by reaction (4) (Figure 4b). The parallel circuit RC is in series with a resistance R2 to represent the pseudocapacitive effect caused by the xanthate adsorption on the surface (CPE2). Finally, R3 represents the second time constant correlated with the onset of chalcopyrite oxidation, reaction (7). An extra resistor is then incorporated in series to represent the solution resistivity, R_s (R1). All the values for the electrical

parameters fitted to experimental data in the equivalent circuit are listed in Table II and the statistical error x^2 is less than 1×10^{-3}. The presence of X^- species has been well identified by spectroscopic techniques on the oxidized chalcopyrite surface during further assessment of chalcopyrite and collectors systems [28-29].
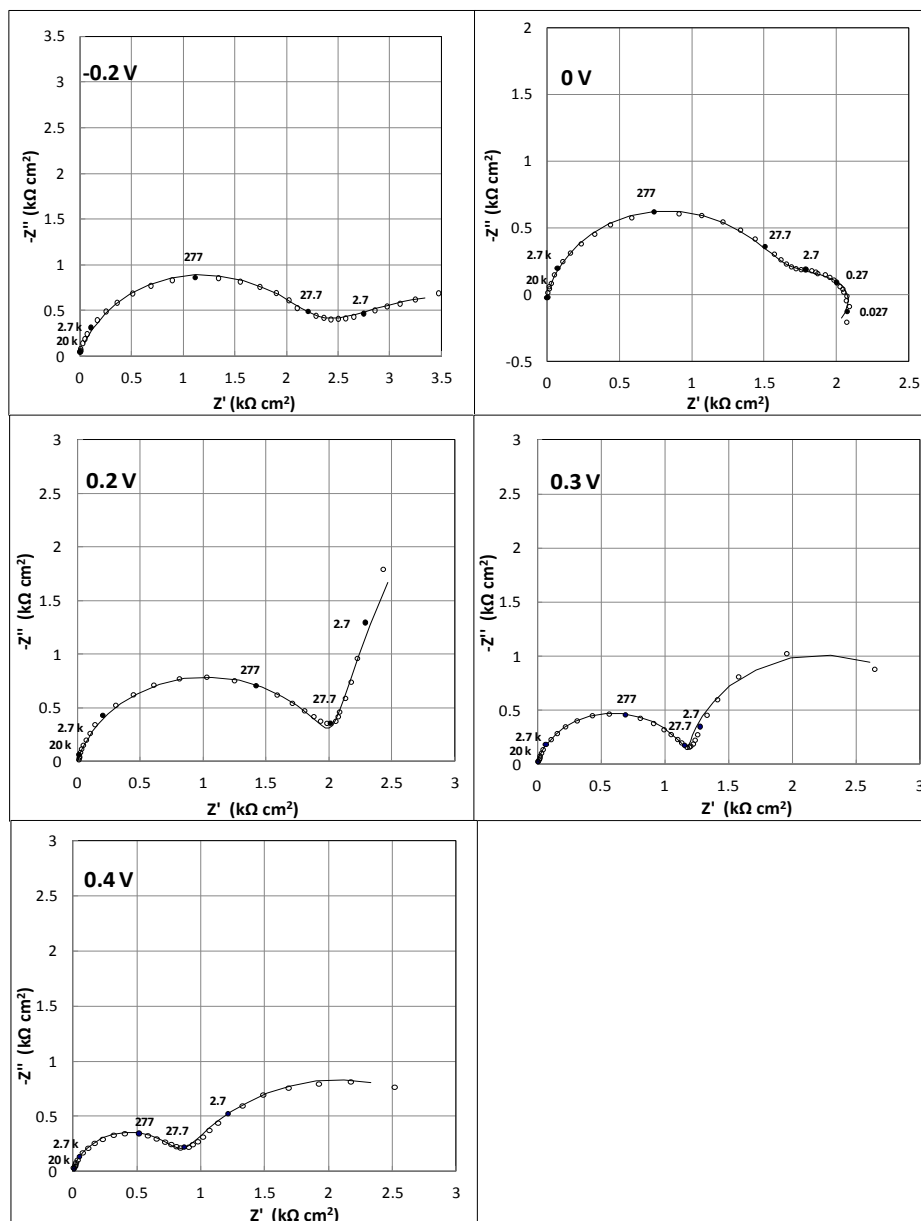
Figure 5. Complex EIS spectra (Nyquist plots) for chalcopyrite system (KCl 0.01 M solution at different polarization potentials) in the presence of different X^- concentrations. Experimental data is shown in open symbols (o). Fitted data is shown in continuous lines. Proposed equivalent circuits are shown in Figure 4a. Frequency in Hertz.

Two time constants are also present for impedance spectra obtained for applied polarization potentials at 0.3 and 0.4 V vs. SCE. However, for these particular cases, the increase in the

polarization potential breaks down the passive stage and reactivates the surface. Therefore, the pseudocapacitance effect observed at the low frequencies range (Fig.5, 0.2 V) disappears. In this regard, the adsorption of xanthate and chalcopyrite oxidation, reactions (4) and (7), are favored. This is further supported by a reduction of the charge transfer resistance R_{CT1} (R2) and R_{CT2} (R3) (Table II). These processes are also represented by the equivalent electrical circuit illustrated in Figure 4b. In a similar direction, the decrease in the double layer differential capacitance suggests a less compact and stable double layer. Finally, we can mention that above a potential 0 V, there are not inductive effects on the system, so we discard the presence of intermediary adsorbed in the interface. This observation is congruent with the cyclic voltammetry results detected after stirring the media (Fig. 1b).

Table II. Electrical parameters obtained by the EIS data fitting for chalcopyrite in occurrence of X-species to the equivalent circuit in Fig 4a-4c.

E (V)	CPE1 ($\mu\Omega cm^{-2} s^n$)	n	$R_{ct1}(k\Omega)$	CPE2 ($m\Omega cm^{-2} s^n$)	n	R_{ct2} (kΩ)	L (H)
-0.2	69	0.835	2.23	4	0.52	2.95	-
0	6.7	0.838	1.59	1.29	0.55	0.54	43.58
0.2	14.17	0.8325	2.05	1.973	0.884	20	-
0.3	12	0.842	1.213	1.75	0.97	2.1	-
0.4	12	0.836	0.912	0.84	0.83	2	-

Natural pyrite (FeS_2) and/or chalcopyrite samples were analyzed by Velásquez et al. [30] afterward electrochemical perturbations accomplished in alkaline borax medium (at pH= 9.2), in order to correlate textural and chemical modifications arising on their mineral surfaces as a result of changes in electrochemical processes of interest for copper extraction methodologies. A methodical study of the further interactions between collector xanthate and oxidized chalcopyrite samples is here performed on the EIS basis in KCl media intending to comprehensively correlate chemical changes and redox processes occurring during electrochemical reactions, covering significant ions and conditions for mining industry and environmental issues, thus allowing extending observations between modified chalcopyrite surfaces including secondary compounds, and collectors behavior based on mechanisms processes of mineral/xanthates systems.

4. CONCLUSIONS

The combination of cyclic voltammetry, double-layer capacitance and EIS characterizations of chalcopyrite, $CuFeS_2$, in the occurrence and/or absence of highly concentrated xanthates solutions has been presented. There were identified the adsorption and desorption of xanthate on chalcopyrite and

the formation of Cu^{2+} and Fe^{2+} species (0-0.3 V) as an overlapped peak, followed by the formation of covallite, CuS (0.8-0.9 V). In addition, double layer capacitance measurements allow us to determine the PZC for the chalcopyrite-xanthate system, $CuFeS_2$-X equal to 0.2 V. Impedance spectra acquired at PZC supported both the adsorptive process of xanthate (X^-) species on the mineral surface and the passivation of the chalcopyrite evidenced by a pseudocapacitive effect. These effects are also correlated with the blocking of oxidized species of Cu^{2+} and Fe^{3+} from the matrix to the surface. A series of equivalent circuits that take into account the different processes involved in the system were proposed. This information provides a better understanding of the interfacial reactions for this system.

References

1. W. Tolley, D. Kotlyar and R. Van Wagoner, *Mineral Engineering*, 9 (1996) 603.
2. G. D. Senior and W. J. Trahar, *Int. J. Miner. Process*, 33 (1991) 321.
3. R. Woods, M. C. Fuerstenau, *In Flotation,* AIME, New York (1976).
4. P. Nowak, *Fyzykochemiczne Problemy Mineralurgii*, 21 (1989) 107.
5. G. Fairthorne, D. Fornasiero, J. Ralston, *J. Miner. Process*, 50 (1997) 227.
6. G. Fairthorne, D. Fornasiero and J. Ralston, *Int. J. Miner. Process*, 46 (1996)137.
7. M. C. Fuerstenau, J. D. Miller, M. C. Kuhn, *Chemistry of Flotation*. AIME, New York, (1985).
8. M. C. Fuerstenau, J. L. Huiatt and M. C. Jun, *Trans. AIME*, 250 (1971) 227.
9. M. C. Fuerstenau, South African Institute of Mining and Metallurgy, Monograph series. Chap. 6, pp. 91-108 (1982).
10. J. R. Gardner and R. Woods, *Int. J. Miner. Process*, 6 (1979) 1.
11. S. A. Allison, L. A. Goold, M. J. Nicol and A. Granville., *Metallurgical Transactions*, 3 (1972) 2613.
12. Richarson and Walker, *Congr. Int. Mineralurgie*, 2 (1985) 198.
13. R. R. Roos, J. P. Celis and A. S. Sudarsono, *Int. J. of Mineral Processing*, 29 (1990a) 17.
14. R. R. Roos and A. S. Sudarsono, *Int. J. of Mineral Processing*, 28 (1990b) 231.
15. J. O. Leppinen, C. I. Basilio and R. H. Ion, *Colloids and Surfaces*, 32 (1988) 113.
16. E. D. Moreno-Medrano, N. Casillas, R. Cruz, R. H. Lara-Castro, M. Bárcena-Soto, E. R. Larios-Durán., *Int. J. Electrochem. Sci*., 6 (2011) 6319.
17. I. V. Chernyshova, *J. Phys. Chem. B*, 105 (2001) 8185.
18. S. Mustafa, A. Hamid and A. Naeem, *Int. J. Miner. Process,* 74 (2004) 317.
19. Q. Yin, D. J. Vaughan, K. E. R. England, G. H. Kelsall and N. P. Brandon, *Journal of The Electrochemical Society,* 147 (2000) 2945.
20. K. N. Mendiratta, *Kinetic Studies of Sulfide Mineral Oxidation and Xanthate Adsortion*, PhD thesis, Blacksburg, Virginia (2000).
21. E. C. Todd, D. M. Sherman, J. A. Purton, *Geochim. Cosmochim. Acta,* 67 (2003) 2137.
22. R. G. Acres, S. L. Harmer, D. A. Beattie, *Int. J. Miner Process*, 94 (2010) 43.
23. T. Güler, C. Hiçyilmaz, G. Gökağaç, Z. Ekmeçi, *Miner Engineer,* 19 (2006) 62.
24. D. C. Grahame, Theory of Electrocapillarity, *Chem. Rev*., 41 (1947) 441.
25. B. E. Conway, R.G. Barradas and T. Zawidzki, *S. Phys. Chem*., 62 (1958) 676.

26. B. B. Damaskin, O. A. Petrii and V. Batrakov, *Adsorption of Organic compounds on electrodes*, Plenum Press, New York (1971).
27. P. Velásquez, H. Gómez, D. Leinen, J. R. Ramos-Barrado, *Colloids Surface A: Physicochem. Eng. Aspects*, 140 (1998) 177.
28. E. Bagci, Z. Ekmekci and D. Bradshaw, *Minerals Engineering*, 20 (2007) 1047.
29. T. Güler, C. Hiçyilmaz, G. Gökağaç and Z. Ekmeçi, *Journal of Colloid and Interface Science,* 279 (2004) 46.
30. P. Velásquez, D. Leinen, J. Pascual, J. R. Ramos-Barrado, P. Grez, H. Gómez, R. Schrebler, R. Del Rio and R. Córdova, *J. Phys. Chem. B,* 109 (2005) 4977.